DOES EAST EURASIAN SNOW COVER TRIGGER THE NORTHERN ANNULAR MODE?

Eun-Jeong Cha and Masahide Kimoto
Center for Climate System Research, University of Tokyo

1. Introduction

A dominant mode of winter climate variability in the North Atlantic region is known as the North Atlantic oscillation (NAO) or Arctic Oscillation (AO; Thompson and Wallace, 1998), a large-scale seesaw in atmospheric mass between middle and high latitudes.

Whatever the dominant mode of NH atmospheric variability is referred to, NAO or AO or Northern Annular Modes (NAM; Limpasuvan and Hartmann 1999), the forcing mechanisms of this dominant atmospheric pattern should be of much academic and practical interest. Although we do not have a particular preference for the nomenclature, we deal extension of NAO in sectors out of North Atlantic and make more frequent use of NAM or AO (indistinguishably) in this article. In general, NAM is recognized as an "internal" mode of the atmosphere, i.e., the atmospheric dynamics acts to sustain the mode and no "external" forcing is required for its existence (DeWeaver and Nigam, 2000; Kimoto et al., 2001). However, transitions and persistence of such a mode can still be subject to conditions "external" to the atmospheric dynamics and it is important for predictability study to identify exact mechanisms in which the atmospheric intrinsic mode is affected by such conditions. With regards to interannual to decadal variability of the NAM pattern, previous studies suggested regional boundary forcings such as sea surface temperatures (Rodwell, 1999), snow cover over the eastern Eurasia in October (Cohen and Entekhabi, 1999; Cohen et al., 2001), or sea ice variability (Mysak and Venegas, 1998) and rather hemispheric-scale forcings such as those originating from the stratosphere after the beginning of November (Baldwin and Dunkerton, 1999) or even aerosols (Perlwitz and Graf, 1995).

In examining one of the forcing mechanisms suggested in the previous paragraph, we caught sight of a typical year of the negative phase of NAM that occurred around November 2000. The subsequent winter was unusually snowy and the cold winter monsoon conditions prevailed over the East Asian countries and lasted for 3 to 4 months. Therefore, the year 2000/01, the higher than normal snow distribution in October 2000 and the NAM-like winter atmospheric circulation of 2000/01, is a good example for reexamining the hypothesis with realistic, observation-based initial conditions.

2. Model and observational data

The weekly snow data sets are obtained from the Climate prediction Center (CPC) of National Oceanic and Atmospheric Administration (NOAA). This CPC product is computed using the Operational Northern Hemisphere Snow Cover Data and is available at the CPC web site (http://www.cpc.ncep.noaa.gov/data/snow/). Time series of daily AO index since 1958 used in this study is found at the website (http://www.atmos.colostate.edu/ao/Data/AO Daily_Index_1958Current.ascii). This index (Thompson et al., 2000) has been constructed by projecting daily SLP anomalies onto the first empirical orthogonal function (EOF) of the NH sea level pressure (SLP). The daily SLP data set is based on the National Centers for Environmental Prediction-National Center for Atmospheric Research (NCEP/NCAR) reanalysis (Kalnay et al., 1996). We use the NCEP/NCAR reanalysis also to depict upper-air anomalies. These data set has a horizontal resolution of $2.5^{o}\times2.5^{o}$ longitude-latitude, except for surface temperature (hereafter Tsfc), which is available on the T62 Gaussian grid ($\sim1.875^{o}\times1.875^{o}$). The global sea surface temperature data provided by the UK Met Office (Parker et al., 1995), referred to as HadISST, is utilized to drive an atmospheric general circulation model. The analysis period adopted in this study is 1973-2001 in which both snow cover and the NCEP/NCAR data are available. An east Eurasian box is defined as region bounded by 40°N and 70°N in latitude, and by 70°E and 140°E meridians.

The atmospheric general circulation model (AGCM) used in this study has been developed jointly by the Center for Climate System Research (CCSR) of the University of Tokyo and the National Institute for Environmental Studies (NIES), hereafter referred to as the CCSR/NIES AGCM. This model is a global spectral model with triangular truncation at wave number 42 and with 20 sigma levels in the vertical. Details of the model formulation are given in Numaguti et al. (1997).

3. Observational data analysis

3.1 Interannual variability of snow in autumn and following winter atmospheric circulation

We examine the lead-lag relationship between the autumnal snow cover over the eastern Eurasia and subsequent wintertime NAM phase in terms of long-term time series. First we plot in Fig. 1a time series of Sep.-Oct.-Nov. (SON) snow cover which is averaged over the east Eurasia region (black solid line with circle), principal components (PCs) (black solid line with cross) of the first mode of empirical orthogonal function (EOF1) of DJF 500 hPa geopotential height, and DJF seasonal mean AO index (red solid line with cross). For the period of 1973-2001, snow cover and EOF1 PCs went through similar but opposite polarity of decadal shifts, maximum and minimum peakings in 1976 and collapsed to record minimum and maximum in 1988, but reached maximum and minimum again in 2000. A more detailed comparison of SON snow cover and DJF EOF1 shows lead-lag linkage for other individual years; the heavy snow years (1976, 1978, 1985, and 2000) correspond to negative PCs years (negative phase of NAM), while the light snow years (1975, 1988, 1989, 1991, 1992, and 1999) correspond to positive PCs years (positive phase of AO). Correlations of the snow with PCs of 500 hPa heights and with DJF AO index are -0.69 and -0.69, respectively.

Next we consider monthly spatial (Fig. 1b) and temporal (Fig. 1c) correlations between SON snow cover over the east Eurasia and DJF 500 hPa geopotential heights in subsequent winters. The monthly lag correlation maps indicate that the annular mode builds up from September although correlation magnitudes are small and not significant. The correlations develop rapidly from October. The pattern shown in Fig. 4.8b consists not only of the local negative correlations over the Eurasian continent but also of remote negative correlations over the northern Europe and North America, and positive correlations over the Arctic Ocean. In November which is similar to those of October, the correlations are much weaker.

The time-lagged correlation coefficients between the monthly snow anomalies over the eastern Eurasia and PCs of the EOF1 DJF 500 hPa height are shown in Fig. 1c. The results represent that the snow is leading the atmospheric anomalies by about two months and is correlated for October and November values. However, the significant lagged correlation relationship between two variables disappears in December and later.

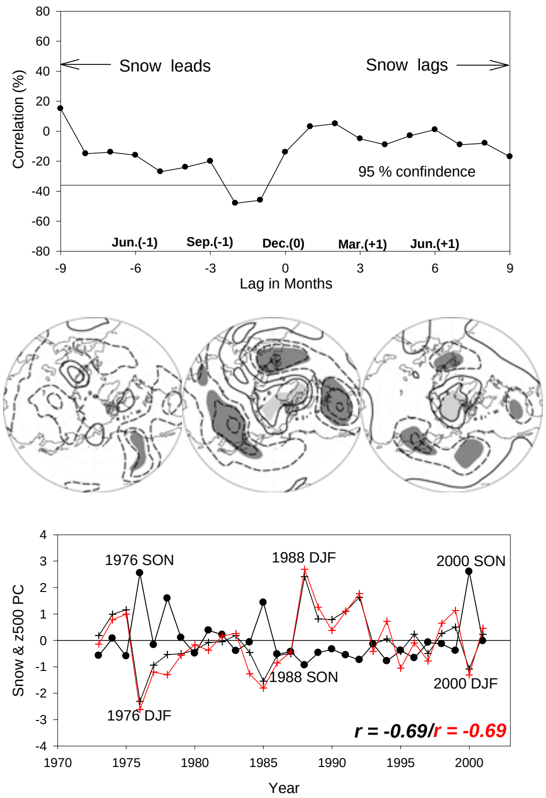

Figure 1.
(a) Time series of the averaged snow cover (black solid line with circle) over the East Eurasia (40°N-70°N, 70°E-140°E) in SON, PCs of EOF1 for DJF 500 hPa geopotential heights (black solid line with cross), and monthly AO index (red solid line with cross), respectively. The correlation coefficients (r) are given at the lower right corner.

(b) Maps of correlation coefficients of 500 hPa geopotential heights in winter with respect to Sep.(left)-Oct.(middle)-Nov.(right) snow cover over the East Eurasia. Contour intervals are %. The map domain begins at 20°N. (c) Lagged correlation between the PCs of EOF1 for DJF 500 geopotential height and snow cover over the East Eurasia. Unit is %. The abscissa represents the lag between the two time series in months; negative when snow leads height. The solid line represents significant at the 95 % level.

3.2 An overview of autumn 2000 (1988) and winter 2000/01 (1988/89)

The October of year 2000 was characterized as a period when large positive anomalies in the Eurasian snow cover were observed. Figure 2a shows October monthly mean snow cover (black solid line) and Tsfc anomalies (shadings) in 2000. Positive snow cover anomalies over the Eurasian Continent covered a broad area of 40°-70°N, 70°-140°E, approximately. Also, there were heavier than normal snow cover anomalies over the Greenland, Alaska, and northern part of Canada. The distinct regional cold Tsfc anomalies (~ -4K) were observed in October 2000 in eastern Eurasia, which corresponded to areas having heavier than normal snow cover. Further to the west, the other cold anomalies extended to the North Africa. The warm anomalies (~ +5K) were situated in northern Europe, the Arctic Ocean, and somewhat less (~ +3K) in the U.S.

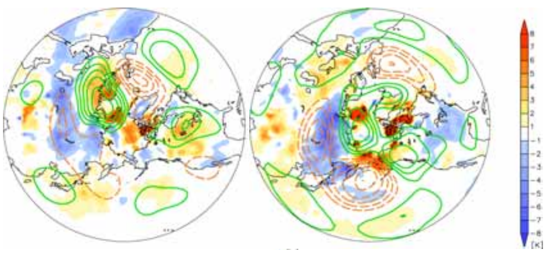

Figure 2.
(a) Snow cover (black solid line), surface air temperature (shading), and 500 hPa geopotential height (contours with color) anomalies observed in October 2000. The values greater than zero of snow covers are denoted by black solid line. Contour interval is 20 m for the geopotential height. (b) 500 hPa geopotential height anomalies observed in winter of 2000/01. Contour interval is 20 m for the geopotential height. Zero contours are suppressed. The map domain begins at 20°N.

Maps of 500 hPa geopotential height (Z_{500}) anomalies during October 2000 are presented in Fig. 2a. The October monthly average of Z_{500} anomalies resembled the Eurasian (EU)-like teleconnection pattern (Wallace and Gutzler, 1981) with alternating positive and negative Z_{500} anomalies from the North Atlantic, across the Eurasian Continent, extending to the Far East Asian coastal areas. The negative Tsfc anomalies observed in eastern Eurasia were associated with the negative height anomalies. In Europe, anomalous positive Tsfc anomalies were observed.

In winter seasonal mean Z_{500} fields (Fig. 2b), positive anomalies were predominant over the Arctic including Greenland, most of North America, eastern Europe and Middle East, while negative anomalies were seen over mid-latitudes, especially the northern Pacific, Eurasia, Mongolia, and mid-latitude band in the Atlantic sector. This Z_{500} anomaly configuration resembled well the NAM pattern (e.g., TW98). Deeper-than-normal Aleutian low continued through the DJF and seasonal-mean Tsfc (shaded) was much lower than normal over most of the eastern Eurasia.

Overall, CRU (1988/89) surface temperature time series (Fig. 4.4) and horizontal distributions (Fig. 4.5b) showed approximately the same as the NCEP/NCAR Tsfc anomaly patterns.

4. Ensemble simulation of the 2000/01 and 1988/89 winter

To investigate the lagged relationship between snow in autumn over the eastern Eurasia and the NAM in winter, a numerical experiment using an AGCM is performed with initial conditions taken from the NCEP/NCAR daily data and by giving prescribed climatological SSTs (Parker et al., 1995) as the lower boundary condition. The sea ice is prescribed by climatology of the Atmospheric Model Intercomparison Project-2 (AMIP2; Gates 1992). The initial conditions are prepared using the NCEP/NCAR reanalysis daily data. Initial snow amount and soil wetness are taken from a 17-year monthly climatology of the present model's AMIP2 integration.

The ensemble experiment consists of 10 independent integrations of about 6-month long starting from 15, 16,…24 October 2000 to the end of April 2001. In addition to the year of 2000/01 ensemble experiments, another set of ensemble integrations, with initial conditions of 15, 16,…24 October 1988 to the end of April 1989, has also been carried out. It is noted that smaller than normal snow cover appeared in October 1988 succeeded by positive 500 hPa height anomalies over the midlatitudes in 1988/1989 winter; namely, the autumnal snow cover and winter 500 hPa height anomalies in 1988/89 were opposite to the those of 2000/01. These contrasting cases have been chosen to examine predictability of the polarity of DJF circulation anomalies by the model.

In the difference between observed surface temperatures from 15~24 October 2000 and those of 1988 obtained from NCEP/CDAS (Fig. 3a), which is employed as the initial condition. We refer to this ensemble experiment as *Intense Snowfall Period* (hereafter, *ISP*). The largest negative anomalies above 8 K are found over the eastern part of the Eurasia. Other minor cooling areas were located over north Canada and a part of Greenland, and warming occurred around the Arctic Ocean and a part of North American Continent.

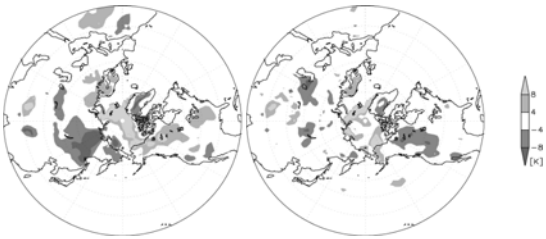

Figure 3.
Difference initial condition (a) 15-24 (ISP) and (b) 5-14 (BISP) of October surface temperature 2000 versus 1988 obtained from NCEP/CDAS daily data. The map domain begins at 20^{o}N.

Figure 4a is the difference of 500 hPa geopotential heights between 2000/01 and 1988/89 DJF of NCEP/CDAS, while Fig. 4b shows the same as Fig. 4a except for the ensemble mean of ISP experiment. At the 500 hPa surface, observed anomalies during winter (Fig. 4a) have characteristics similar to the annular mode: the dipole pattern between the negative anomalies over the midlatitudes and positive anomalies in polar region. The model generally succeeds in generating consistent features of the 500 hPa heights, such as dipole anomalies except for the features over the North Atlantic. It is noteworthy that Fig. 4b shows a negative area in eastern Eurasia and North Pacific and positive polar region has significant anomalies (denoted by shading) at the 95 % level although its magnitude is smaller than those of observations.

The good agreement with observations demonstrates the model's capability in capturing the important circulation anomalies over the Eurasia sector during 2000/01 winter months. However, there are several disagreements between the observed height anomalies and ensemble mean results that cannot be ignored. In particular, the amplitude of the height response is somewhat weak than observed anomalies. In addition, simulated height difference over the North Atlantic is somewhat distorted and shifted eastward. The discrepancy between the observation and model result over the Atlantic sector was also reported by WN99.

In order to assess the dependence of the above results on the initial condition, another set of ensemble integrations has been made conditions between 5 and 14 October (Fig. 3b), which is referred as *B*efore the *I*ntense *S*nowfall *P*eriod (hereafter, *BISP*) in 2000 and 1988. The most notable difference between ISP and BISP initial conditions shown in Figs. 3a and b is that no cold Tsfc signal can be found over the eastern Eurasia. Instead, rather weak warm conditions in BISP experiments in contrast with ISP experiments. Figure 4c shows the ensemble mean anomalies of 500 hPa heights forced by the initial conditions shown in Fig. 3b. Anomalies are much weaker and disorganized in comparison with Fig. 4b, and most importantly there is no sign of the negative NAM configuration. This result further supports the idea that the cold initial condition over the East Eurasia is strongly contributed to the formation for NAM.

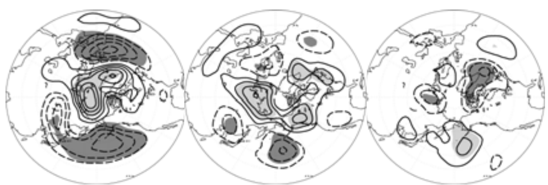

Figure 4.
Difference of DJF 500 hPa geopotential height anomalies 2000 versus 1988 (a) NCEP/CDAS, (b) result of the AGCM experiment with ISP, and (c) result of the AGCM experiment with BISP, respectively. Zero contours are removed. Contour intervals are 40 m in (a) and 10 m in (b) and (c). Coefficients that are significant at the 95 % confidence level are shaded. The map domain begins at 20^{o}N.

5. Summary and concluding remarks

East Asian countries experienced record-breaking cold waves during the winter season of 2000/01. The 500 hPa height during 2000 DJF in the NH was characterized by the annular mode with positive anomaly covering the Arctic and negative anomaly over the midlatitudes. This annular mode was likely to be triggered by heavier snow in autumn snow cover in October 2000 over the eastern Eurasia and might be contributed the surface unusual cold winter over the East Asian countries during winter of 2000/01. This study documents and analyzes the unusual large-scale circulation of 2000/01 winter associated with cold surface condition over the eastern Eurasia in October 2000.

The height anomalies at 500 hPa (Z_{500}) were characterized by EU-like pattern in October 2000. At winter seasonal-mean 500 hPa height fields, positive anomalies were predominant over the Arctic including Greenland, most of North America, eastern Europe and Middle East while negative anomalies were over mid-latitudes, especially the northern Pacific, Eurasia and Mongolia, and mid-latitude band over the Atlantic. This Z_{500} anomaly configuration resembled well the NAM and was strongly negative in this winter. The enhanced vertical wave activity flux propagation took place over the cold surface from October 2000.

According to the long term statistical analysis, snow leads the annular mode of atmospheric variability in NH for approximately 2 months. The SON snow cover over the East Eurasia and EOF1 of DJF 500 hPa heights are highly correlated during 1973-2001.

The monthly lag correlation maps indicate that the annular mode builds up from September and the correlations develop rapidly from October with negative correlations over the northern Europe and North America, and positive correlations over the Arctic Ocean.

An AGCM hindcast experiment with October 2000 and 1988 initial conditions obtained from NCEP/CDAS has been carried out. The polarity between the polar region and midlatitues is reproduced qualitatively by the simulation which started after the intensive snowfall period in October 2000 (or vice versa in 1988), except for the features over the North Atlantic. But, the experiment which started from the period before the intensive snowfall period fails to reproduce the NAM.

The implication of the model result is that only the initial condition can generate the annular mode which can be predicted with 2-month leading time for following winter. This is potentially an important implication for successful extended weather forecasts for the cold season.

References

Baldwin, M. P., and T. J. Dunkerton, 1999: Propagation of the Arctic oscillation from the stratosphere to the troposphere. *J. Geophys. Res.*, **104** (D24), 30 937-30 946.

Cohen, J., and D. Entekhabi, 1999: Eurasian snow cover variability and Northern Hemisphere climate predictability. *Geophys. Res. Lett.*, **26**, 345-348.

Cohen, J., K. Saito, and D. Entekhabi, 2001: The role of the Siberian high in the Northern Hemisphere climate variability. *Geophys. Res. Lett.*, **28**, 299-302.

DeWeaver, E., and S. Nigam, 2000: Zonal-eddy dynamics of the North Atlantic oscillation. *J. Climate*, **13,** 3893-3914.

Kalnay, E., and Coauthors, 1996: The NCEP/NCAR Reanalysis Project. *Bull. Amer. Meteor. Soc.*, **77**, 437-471.

Kimoto, M., F.-F., Jin, M. Watanabe, and N. Yasutomi, 2001: Zonal-eddy coupling and a neutral mode theory for the Arctic Oscillation. *Geophys. Res. Lett.*, **28,** 737-740.

Limpasuvan, V., and D. L. Hartmann, 1999: Eddies and the annular modes of climate variability. *Geophys. Res. Lett.*, **26**, 3133-3136.

Mysak, L. A., and S. A. Venegas, 1998: Decadal climate oscillations in the Arctic: A new feedback loop for atmosphere-ice-ocean interactions. *Geophys. Res. Lett.*, **25,** 3607-3610.

Numaguti, A., S. Sugata, M. Takahashi, T. Nakajima and A. Sumi, 1997: Study on the Climate System and Mass Transport by a Climate Model. *CGER's supercomputer monograph report*, National Institute for Environmental Research, Environment Agency of Japan, **3**, 91 pp.

Parker, D. E., C. K. Folland, A. Bevan, M. N. Ward, M. Jackson, and K. Maskell (1995), Marine surface data for analysis of climatic fluctuations on interannual to century timescales. *Natural Climate Variability on Decade to Century Time Scales*, D. G. Martinson et al., Eds., National Academy Press, 241-250.

Rodwell, M. J., D. P. Rowell, and C. K. Folland, 1999: Oceanic forcing of the wintertime North Atlantic oscillation and European climate. *Nature*, **398,** 320-323.

Thompson, D. W. J., and J. M. Wallace, 1998: The Arctic Oscillation signature in the wintertime geopotential height and temperature fields. *Geophys. Res. Lett.*, **25**, 1297-1300.

Thompson, D. W. J., J. M. Wallace and C. G. Hegerl, 2000: Annular modes in the extratropical circulation. Part Ⅱ: Trends. *J. Climate,* **13**, 1018-1036.

Wallace, J. M., and D. S. Gutzler, 1981: Teleconnections in the geopotential height field during the Northern Hemisphere winter. *Mon. Wea. Rev.*, **109**, 784-812.

Watanabe, M., and T. Nitta, 1998: Relative impacts of snow and sea surface temperature anomalies on an extreme phase in the winter atmospheric circulation. *J. Climate*, **11**, 2837-2857.

Watanabe, M., and T. Nitta, 1999: Decadal change in the atmospheric circulation and associated surface climate variation in the Northern Hemisphere winter. *J. Climate,* **12**, 494-510.